

## Room- and High-Pressure Neutron Structure Determination of Tetrathiafulvalene–7,7,8,8-Tetracyano-*p*-quinodimethane (TTF–TCNQ). Thermal Expansion and Isothermal Compressibility

BY ALAIN FILHOL

*Laboratoire de Cristallographie et de Physique Cristalline, LA CNRS n° 144, Université de Bordeaux I, 351 cours de la Libération, 33405 Talence, France and Institut Laue–Langevin, 156 X Centre de Tri, 38042 Grenoble CEDEX, France*

GEORGES BRAVIC, JACQUES GAULTIER AND DANIEL CHASSEAU

*Laboratoire de Cristallographie et de Physique Cristalline, LA CNRS n° 144, Université de Bordeaux I, 351 cours de la Libération, 33405 Talence, France*

AND CHRISTIAN VETTIER

*Institut Laue–Langevin, 156 X Centre de Tri, 38042 Grenoble CEDEX, France*

(Received 30 August 1980; accepted 1 December 1980)

### Abstract

The TTF–TCNQ structures at  $10^{-1}$  and  $4.6 \times 10^2$  MPa have been refined to  $R = 0.046$  from full sets of intensities (1084 and 1141 independent reflections respectively) up to  $\sin \theta/\lambda = 0.59 \text{ \AA}^{-1}$ . The space group is  $P2_1/c$  and cell dimensions are at  $10^{-1}$  MPa:  $a = 12.291$  (6),  $b = 3.825$  (2),  $c = 18.425$  (10) Å,  $\beta = 104.49$  (5)°; and at  $4.6 \times 10^2$  MPa:  $a = 12.188$  (6),  $b = 3.741$  (2),  $c = 18.307$  (10) Å,  $\beta = 104.27$  (5)°. An increase of the charge transfer by 10% for  $4.6 \times 10^2$  MPa has been estimated from the change in intramolecular bond lengths. The major effect of pressure on the crystal packing is the change in the stacking distance in the columns of TTF molecules [3.476 (2) to 3.417 (1) Å] and of TCNQ molecules [3.170 (3) to 3.104 (2) Å] while reorientational movements are small. The isothermal compressibility and the thermal expansion of TTF–TCNQ have been measured, leading to results in partial disagreement with some published earlier. The anisotropies and directions of principal compressibilities and thermal expansion have been calculated and explained by means of a simple model based on structural considerations.

### Introduction

The organic charge-transfer salt TTF–TCNQ (tetrathiafulvalene–tetracyano-*p*-quinodimethane) is well known for its quasi one-dimensional electronic-transport properties and its sequences of Peierls and collective phase transitions at low temperature. Its

physical properties have thus been the subject of detailed studies as a function of various physical conditions, among which pressure changes have proved to be very instructive (Friend, Miljak & Jérôme, 1978).

The structure of TTF–TCNQ is known at several temperatures in the range 40 to 300 K (Kistenmacher, Phillips & Cowan, 1974; Blessing & Coppens, 1974; Schultz, Stucky, Blessing & Coppens, 1976) but no high-pressure structure determination has previously been performed. Also, several papers include calculations using thermal-expansion and isothermal-compressibility data but, as shown by Megtert, Comès, Vettier, Pynn & Garito (1979), the estimation of compressibility can be of questionable accuracy.

Therefore, in the present paper, the neutron structure of TTF–TCNQ at ambient pressure and at  $4.6 \times 10^2$  MPa is described. In addition, new data about the cell dimensions as a function of pressure and temperature are given.

### Experimental

Neutron diffraction measurements were carried out on the D8 four-circle diffractometer located on a thermal beam tube at the high-flux reactor of the Institut Laue–Langevin at Grenoble. The incident neutron beam had a wavelength  $\lambda = 1.2690$  (5) Å [Cu(200) monochromator] with a flux at the sample position of about  $5 \times 10^5 \text{ n mm}^{-2} \text{ s}^{-1}$  and measured  $\lambda/2$  contamination  $F_{hkl}^2(\lambda/2)/F_{hkl}^2(\lambda) = 0.0028$  (5).

All measurements were carried out at room temperature. The pressure vessel (Paureau, 1980; Paureau &

Vettier, 1975) was made of high-strength Al alloy (AZ8GU) with inside and outside diameters of 10 and 30 mm, respectively, at the sample position. The cell was pressurized with helium gas; during the experiment the pressure stability was measured with strain gauges mounted on the outside of the cell. These had

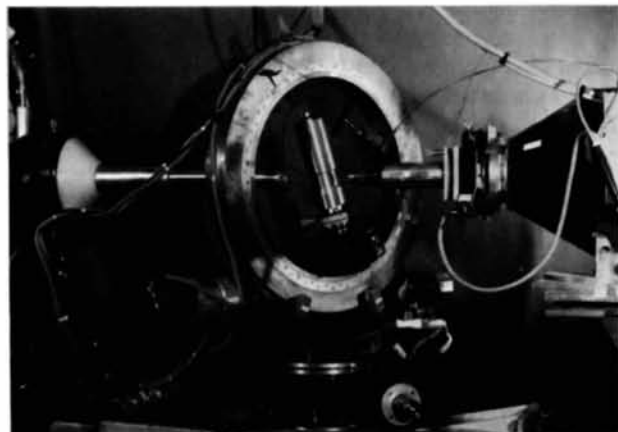


Fig. 1. The high-pressure cell mounted on the D8 neutron four-circle diffractometer of the ILL.

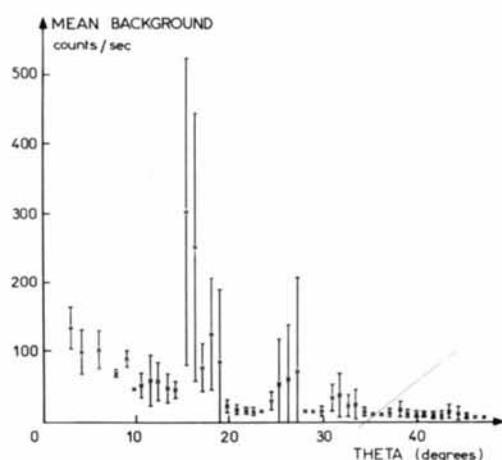


Fig. 2. Mean background as a function of Bragg angle  $\theta$ . Each point of the plot is the observed background level averaged over all reflections lying in the corresponding  $\theta$  range. The error bars give the e.s.d. of the observed distribution.

been calibrated against manganin sensors in the piston assembly used to pressurize the cell. To the sensitivity ( $\pm 5.0$  MPa) of the gauges mounted on the cell, no leak could be detected.

The cell was surrounded by an Al-alloy shield with outside diameter 60 mm. The cell and its shield were mounted on the  $\phi$  table of the Eulerian cradle of the diffractometer with a cell holder providing  $x, y, z$  degrees of freedom (Fig. 1). A pressure valve was attached to the cradle and the capillary tubing connecting it to the cell made a  $360^\circ$  rotation in  $\phi$  possible. Furthermore, it was found unnecessary to dismount the capillary tubing connecting the valve to the pressure intensifier even though this connection is only used for the initial pressurization of the cell. The whole assembly introduced no angular blind spots additional to those of the diffractometer itself.

The major effects on measurements of the introduction of about 40 mm of Al alloys in the beam was, first, to reduce the neutron beam flux (by about 35% at  $1.269 \text{ \AA}$ ) and, second, to produce powder lines which strongly increased the background in limited ranges of angles (Fig. 2).

The sample was a deuterated single crystal ( $2.9 \times 4.3 \times 0.16$  mm) grown from acetonitrile solution. It had the usual form of a platelet elongated along the  $[010]$  chain direction and parallel to the  $(001)$  crystallographic plane. No twinning could be observed. The sample was glued on top of a thin Cd pin which was used as a reference for a rough photographic centring of the sample. The final centring of the sample was achieved by crystallographic methods.

The lattice parameters at five pressures in the range  $10^{-1}$  to  $4.6 \times 10^2$  MPa (Table 1) were determined by least squares from the angular settings of 17 to 26 strong centred reflections.

The lattice parameters at nine temperatures (64 to 293 K) and room pressure (Table 1) were also measured. For this extra experiment, the sample was mounted in a Displex 1003C closed-cycle cryorefrigerator installed on the  $\phi$  circle of the Eulerian cradle of the diffractometer (Allibon, Filhol, Lehmann, Mason & Simms, 1981). Attempts were made to measure the cell dimensions of the low-temperature

Table 1. Cell dimensions as a function of temperature and pressure

The cell parameters have been determined by least squares from the angular settings of 17 to 26 centred reflections. The e.s.d.'s given in parentheses do not include the uncertainty in the wavelength ( $\lambda$ ), this latter being given separately.

$$\lambda = 1.2686 (5) \text{ \AA}$$

$T$ (K)	293	240	199	159	119	90	79	72	64
$P = 10^{-1}$ MPa	$\pm 1$	$\pm 2$	$\pm 1$						
$a$ (Å)	12.286 (2)	12.268 (2)	12.249 (2)	12.237 (2)	12.224 (2)	12.216 (1)	12.216 (2)	12.216 (2)	12.213 (1)
$b$ (Å)	3.827 (1)	3.797 (1)	3.782 (1)	3.763 (1)	3.751 (2)	3.742 (1)	3.738 (1)	3.737 (1)	3.7345 (9)
$c$ (Å)	18.429 (4)	18.407 (5)	18.384 (3)	18.376 (3)	18.361 (5)	18.359 (3)	18.351 (3)	18.350 (4)	18.347 (3)
$\beta$ ( $^\circ$ )	104.51 (2)	104.50 (2)	104.46 (1)	104.44 (2)	104.44 (2)	104.41 (1)	104.40 (1)	104.42 (2)	104.39 (1)
$V$ (Å <sup>3</sup> )	838.9	830.2	824.6	819.4	815.3	812.8	811.7	811.4	810.5
$\rho$ (Mg m <sup>-3</sup> )	1.648	1.665	1.677	1.687	1.696	1.701	1.703	1.704	1.706

Table 1 (*cont.*)

$\lambda = 1.2690$ (5) Å					
$T = 300$ K					
$P$ ( $\times 10^2$ MPa)	0.001	1.02 (5)	2.32 (5)	3.57 (5)	4.6 (5)
$a$ (Å)	12.291 (1)	12.269 (1)	12.239 (1)	12.210 (1)	12.188 (1)
$b$ (Å)	3.8245 (8)	3.8029 (11)	3.7776 (6)	3.7555 (11)	3.7407 (7)
$c$ (Å)	18.425 (4)	18.403 (2)	18.366 (3)	18.335 (2)	18.307 (3)
$\beta$ (°)	104.49 (1)	104.44 (1)	104.38 (1)	104.32 (1)	104.27 (1)
$V$ (Å <sup>3</sup> )	838.5	831.5	822.5	814.7	808.9
$\rho$ (Mg m <sup>-3</sup> )	1.649	1.663	1.681	1.697	1.709

phases but the temperature became unstable below 60 K.

The intensities of Bragg reflections were obtained by means of  $\omega$  scans of 41 steps, the scan width being an experimental function of the Bragg angle  $\theta$ . Apertures before and after the sample were chosen to minimize background and tests on a number of strong reflections showed that there was no intensity loss. The intensity measurements were performed for reflections within the range  $0 < \sin \theta / \lambda < 0.586$  Å<sup>-1</sup> at standard pressure  $P = 10^{-1}$  MPa (the crystal being in the pressure cell) and then at  $P = 4.6 \times 10^2$  MPa.

The data reduction was performed by *COLLSI* of the Institut Laue–Langevin (ILL) which displays the profile of each reflection and allows interactive adjustment of the peak–background separation. Intensities were corrected for the Lorentz factor and the dead-time ( $7 \times 10^{-6}$  s) of the detector.

To correct data for neutron absorption by the pressure cell, the following formula (Albertsson, Oskarsson & Ståhl, 1978), was used:  $I_o = I_{\text{corr}} \times t$  with  $\log(t) = \log(t_0) \times (1 - \sin^2 \theta \sin^2 \chi)^{-1/2}$ , where  $t$  is the transmission factor of the walls and  $t_0$  is the value of  $t$  when  $\chi = 0^\circ$ . By comparing two sets of intensities measured, one from the sample alone, the other from the sample mounted in the pressure cell,  $t_0$  was found to be 0.65 (2). In fact, another value of  $t_0$ , lower by about 9%, had to be used to correct the intensities of some reflections which were measured outside the angular aperture (90°) of the window (5 mm thick instead of 9 mm elsewhere) of the shielding (Fig. 1) of the pressure cell. The minimum transmission factor thus obtained was 0.48. The observed absorption coefficient [ $\mu_o = 0.056$  (5),  $\mu_c = 0.051$  mm<sup>-1</sup>] obtained from transmission measurements over several samples was used to correct intensities for absorption of neutrons by the sample itself (*ABSCOR* of XRAY 74; Stewart, 1974). The absorption was found to be in the range 0.5 to 7.7%.

Finally, intensities of the 1932 and 1855 reflections (including 6% of test reflections) measured at  $10^{-1}$  and  $4.6 \times 10^2$  MPa, respectively, were averaged over equivalent reflections and the agreement factor:  $R = \sum |F_o^2 - \langle F_o^2 \rangle| / \sum F_o^2$  was calculated. The number of independent reflections ( $F_o^2 > 0$ ) thus obtained is 1252 ( $R = 0.0113$ ) for  $P = 10^{-1}$  MPa and 1303 ( $R = 0.0113$ ) for  $P = 4.6 \times 10^2$  MPa, respectively.

At room pressure and room temperature it has been shown from X-ray measurements (Kistenmacher *et al.*, 1974) that TTF–TCNQ crystals have the space group  $P2_1/c$ . For both neutron experiments ( $10^{-1}$ ,  $4.6 \times 10^2$  MPa) the intensities of systematically extinct reflections of the  $P2_1/c$  space group ( $h0l$  with  $l = 2n$  and  $0k0$  with  $k = 2n$ ) were checked.

At  $10^{-1}$  MPa, all  $P2_1/c$  systematically extinct reflections have measured intensities  $I < 3\sigma(I)$  except for the 003 reflection. In this case the ratio  $F_o^2(003)/F_o^2(006) = 0.0025$  (5) corresponds to the  $\lambda/2$  contamination. At  $4.6 \times 10^2$  MPa, four  $P2_1/c$  systematically extinct reflections (003, 009, 305,  $\bar{5}, 0, 19$ ) were found to have significant intensities.  $\lambda/2$  contamination was checked and the following ratios were obtained:  $F_o^2(003)/F_o^2(006) = 0.0028$  (5),  $F_o^2(009)/F_o^2(0, 0, 18) = 0.9$  (2),  $F_o^2(305)/F_o^2(6, 0, 10) = 0.010$  (3); the  $\bar{1}0, 0, 38$  reflection could not be measured. Though the 009 intensity cannot be accounted for by  $\lambda/2$  contamination, the four reflections are all so weak that, for the present, we accept  $P2_1/c$  as the space group of the structure at  $4.6 \times 10^2$  MPa. Further measurements (multiple-scattering test and/or higher pressure) would be needed to elucidate these non-zero intensities.

Another point of interest is that the mosaic spread of the crystal was found to be slightly larger at  $4.6 \times 10^2$  than at  $10^{-1}$  MPa. This effect is larger in the  $[0k0]$  direction than in the  $[h00]$  and  $[00l]$  directions and is reversible. No measurements were made at intermediate pressures. It should be noted that the applied pressure is truly hydrostatic. A possible cause of straining might be the difference in the compressibilities of TTF–TCNQ and the glue (a rubber material) used to mount the sample.

### Structure determination

Structure determinations were carried out in the same way for the  $10^{-1}$  and  $4.6 \times 10^2$  MPa data. Atomic positions given by Kistenmacher *et al.* (1974) were used as starting values. Wilson plots yield the values 1.44 and 1.08 Å<sup>2</sup> for the overall thermal parameters at  $10^{-1}$  and  $4.6 \times 10^2$  MPa respectively.

Table 2. *Refinement data*

$C_6D_4S_4 \cdot C_{12}D_4N_4$ , $M_r = 416.5$ , monoclinic, $P2_1/c$ , $Z = 2$		
$F(000) = 44.4 \times 10^{-11}$ mm		
Scattering lengths (fm) of elements: $b_C = 6.65$ , $b_N = 9.40$ , $b_S = 2.85$ , $b_D = 6.67$		
Linear absorption coefficient for neutrons ( $\lambda = 1.27$ Å):		
$\mu_o = 0.053$ (5) mm <sup>-1</sup>		
Structure refinements	$10^{-1}$ MPa	$4.6 \times 10^2$ MPa
Independent reflections		
Total number	1252	1303
Number with $F_o > 3\sigma(F_o)$	1084	1141
$R = [\sum ( F_o  -  F_c )^2 / \sum F_o^2]^{1/2}$	0.046	0.046

Least-squares refinement (block-diagonal matrix) based on  $F_o$  was used (Table 2). Only reflections with  $|F_o| > 3\sigma(F_o)$  were taken into account; the weighting scheme was  $\sqrt{w} = 1$  if  $|F_o| < P_1$  and  $\sqrt{w} = P_1/F_o$  if  $|F_o| > P_1$  with  $P_1 = |F_o(\text{max.})|/3$ ;  $R = [\sum (|F_o| - |F_c|)^2 / \sum F_o^2]^{1/2}$ .

Refinements, including anisotropic thermal parameters for all the atoms, converged to  $R = 0.046$  for the two pressures. No extinction correction was made. The final values of the atomic coordinates are given in Table 3.\* Bond lengths and angles are displayed in Fig. 3. An ORTEP plot (Johnson, 1965) of the molecule is shown in Fig. 4.

\* Lists of structure factors and anisotropic thermal parameters obtained at both pressures have been deposited with the British Library Lending Division as Supplementary Publication No. SUP 35915 (18 pp.). Copies may be obtained through The Executive Secretary, International Union of Crystallography, 5 Abbey Square, Chester CH1 2HU, England.

Table 3. Fractional coordinates ( $\times 10^4$ ) and equivalent isotropic temperature factors ( $\text{\AA}^2$ ) of the atoms for fully deuterated TTF-TCNQ

First line:  $10^{-1}$  MPa; second line  $4.6 \times 10^2$  MPa. E.s.d.'s are given in parentheses.

$$B_{\text{eq}} = \frac{1}{3} \sum_i \sum_j \beta_{ij} \mathbf{a}_i \cdot \mathbf{a}_j$$

	<i>x</i>	<i>y</i>	<i>z</i>	$B_{\text{eq}}$
S(1)	-932 (5)	-1844 (19)	790 (4)	1.40
	-944 (4)	-1813 (17)	802 (3)	1.24
S(2)	1472 (5)	-1824 (20)	850 (4)	1.49
	1479 (4)	-1815 (17)	853 (3)	1.27
N(1)	3854 (2)	5914 (7)	1901 (1)	2.91
	3834 (2)	6015 (6)	1912 (1)	2.62
N(2)	7483 (2)	6211 (7)	1901 (1)	2.76
	7502 (1)	6319 (6)	1907 (1)	2.46
C(1)	-20 (2)	-3394 (9)	1592 (2)	2.14
	-26 (2)	-3398 (7)	1610 (1)	1.82
C(2)	1080 (2)	-3402 (9)	1621 (2)	2.03
	1085 (2)	-3387 (7)	1637 (1)	1.82
C(3)	113 (2)	-778 (7)	347 (2)	1.57
	116 (2)	-786 (7)	352 (1)	1.41
C(4)	4596 (2)	5090 (8)	1656 (1)	1.69
	4584 (2)	5177 (7)	1667 (1)	1.43
C(5)	6575 (2)	5240 (8)	1659 (1)	1.58
	6581 (2)	5339 (7)	1667 (1)	1.42
C(6)	5469 (2)	4078 (7)	1320 (1)	1.30
	5467 (2)	4165 (6)	1331 (1)	1.16
C(7)	5240 (2)	2043 (7)	667 (1)	1.11
	5236 (2)	2076 (6)	673 (1)	1.02
C(8)	4117 (2)	921 (7)	316 (1)	1.31
	4104 (2)	951 (6)	320 (1)	1.18
C(9)	6109 (2)	1038 (7)	320 (1)	1.34
	6120 (2)	1063 (6)	322 (1)	1.14
D(1)	-391 (4)	-4373 (16)	2027 (3)	5.43
	-410 (4)	-4344 (14)	2052 (2)	4.83
D(2)	1740 (4)	-4350 (16)	2088 (3)	5.43
	1757 (3)	-4353 (14)	2106 (2)	4.82
D(8)	3446 (3)	1656 (11)	570 (2)	3.51
	3427 (2)	1700 (10)	575 (2)	3.15
D(9)	6961 (3)	1855 (11)	576 (2)	3.41
	6979 (2)	1894 (10)	577 (2)	3.15

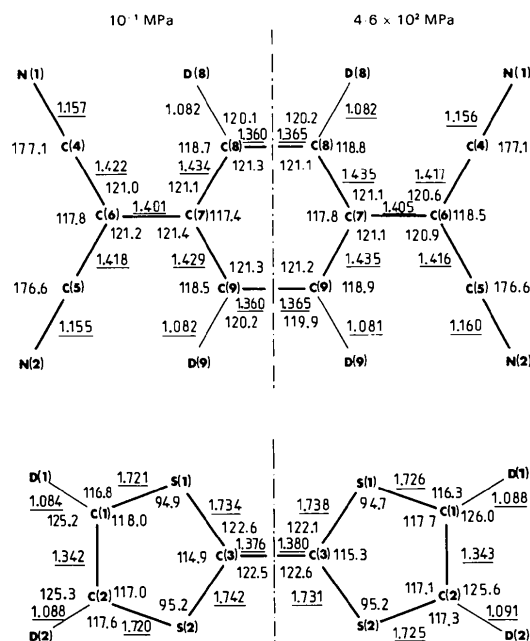


Fig. 3. Bond lengths ( $\text{\AA}$ ) and angles ( $^\circ$ ). Values given here are uncorrected for the riding model. Mean e.s.d.'s for the bond lengths at  $10^{-1}$  and  $4.6 \times 10^2$  MPa are: 0.006 and 0.005  $\text{\AA}$  (C-D), 0.008 and 0.007  $\text{\AA}$  (C-S), and 0.004 and 0.003  $\text{\AA}$  (C-C, C-N). Mean e.s.d.'s for angles (both  $10^{-1}$  and  $4.6 \times 10^2$  MPa) are: TCNQ 0.2, TTF 0.3, and 0.5 $^\circ$  if D atoms are concerned.

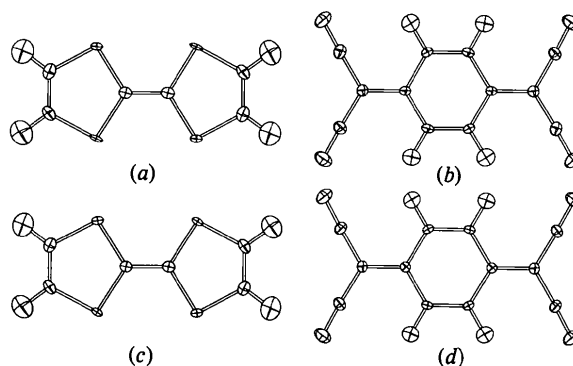


Fig. 4. Thermal-ellipsoid plots (50% probability) of TTF and TCNQ at  $10^{-1}$  and  $4.6 \times 10^2$  MPa. (a) TTF, (b) TCNQ at  $10^{-1}$  MPa; (c) TTF, (d) TCNQ at  $4.6 \times 10^2$  MPa.

#### Description of the structures at $10^{-1}$ and $4.6 \times 10^2$ MPa

For molecular crystals, in the absence of phase transitions, some of the effects on structural parameters of external influences such as temperature or pressure are comparable to the experimental accuracy. For this reason, the experimental data collection and the structure refinements were carried out in the same way at  $10^{-1}$  and  $4.6 \times 10^2$  MPa, to minimize the importance of any systematic errors.

We will describe the effects of pressure on the TCNQ molecule and then on the TTF molecule.

### (i) TCNQ molecule

At room pressure, the bond lengths and angles of the TCNQ molecule are in agreement with the results of the X-ray study by Kistenmacher *et al.* (1974); neutron diffraction yields less scattered results for chemically equivalent bonds. The effect of hydrostatic pressure (Fig. 3 and Table 4) is weak. However, as discussed below, it is sufficient to show the existence of a modification of the charge transfer similar to that observed by Megtert *et al.* (1979) at low temperature.

Neither at room pressure nor at  $4.6 \times 10^2$  MPa is the TCNQ ion strictly planar (Table 5). The quinonoid ring almost has symmetry *m* (or even *mmm* to the accuracy of the data) although the ring is less planar at high pressure. The cyanomethylene groups of one end of the molecule are perceptibly out of this plane with deviations of about 0.05 and 0.08 Å for N(1) and N(2). The angle between mean planes of the ring and of a group  $C(C\equiv N)_2$  is  $2.9 (2)^\circ$ .

The atomic thermal ellipsoids (Fig. 4) are similar in shape and orientation for both pressures but their  $U_{ij}$  factors are smaller by 9% on average at  $4.6 \times 10^2$  MPa. The X-ray data at 100 K (Blessing & Coppens, 1974) and at 60 K (Schultz *et al.*, 1976) gave ellipsoids elongated in the direction of adjacent bonds for C(4) and C(5). This anomaly does not exist in the neutron data.

### (ii) TTF molecule

The bond lengths and angles (Fig. 3), at both pressures, are in close agreement. Some differences may be observed between neutron and X-ray data at room temperature and room pressure: (1) a discrepancy of up to 0.02 Å between mean values of chemically equivalent bond lengths; (2) the neutron

Table 4. Bond lengths (Å) and angles ( $^\circ$ ) averaged over assumed *mmm* symmetry for the TTF and the TCNQ molecules

	10 <sup>-1</sup> MPa	4.6 × 10 <sup>2</sup> MPa		10 <sup>-1</sup> MPa	4.6 × 10 <sup>2</sup> MPa
<i>a</i>	1.376 (4) Å	1.380 (3) Å	<i>a</i>	1.360 (3) Å	1.365 (2) Å
<i>b</i>	1.738 (6)	1.736 (5)	<i>b</i>	1.432 (3)	1.435 (2)
<i>c</i>	1.721 (6)	1.726 (5)	<i>c</i>	1.401 (3)	1.405 (2)
<i>d</i>	1.342 (4)	1.343 (3)	<i>d</i>	1.420 (3)	1.417 (2)
$\alpha$	122.6 (2) $^\circ$	122.4 (2) $^\circ$	<i>e</i>	1.156 (3)	1.158 (2)
$\beta$	114.9 (2)	115.3 (2)	$\alpha$	121.3 (2) $^\circ$	121.2 (2) $^\circ$
$\gamma$	95.1 (2)	95.0 (2)	$\beta$	117.4 (2)	117.8 (2)
$\delta$	117.5 (2)	117.4 (2)	$\gamma$	117.8 (2)	118.5 (2)
			$\delta$	176.9 (2)	176.9 (2)

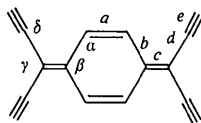
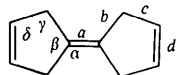


Table 5. Least-squares mean planes and out-of-plane distances (Å) for groups of atoms in TTF-TCNQ at  $10^{-1}$  and  $4.6 \times 10^2$  MPa

In each of the equations of the planes,  $X, Y, Z$  are coordinates (Å) referred to the unit orthogonal axes along  $\mathbf{a}$ ,  $\mathbf{b}$  and  $\mathbf{c}^*$ . The plane equations have the form  $AX + BY + CZ = D$  and the coefficients given below are  $\times 10^4$ . The atoms used to define the plane have been weighted equally. The out-of-plane distance is given for each atom, first for the  $10^{-1}$  MPa structure, then for the  $4.6 \times 10^2$  MPa structure. The e.s.d.'s calculated according to the formulae of Waser, Marsh & Cordes (1973) are given in parentheses.

#### (a) TCNQ

	A	B	C	D	$\chi^2$
P1: mean molecular plane (non-deuterium atoms)					
10 <sup>-1</sup> MPa					
	192 (4)	-8288 (2)	5593	1182 (28)	857
4.6 × 10 <sup>2</sup> MPa					
	202 (4)	-8299 (2)	5576	1230 (24)	1248
N(1)	-0.022 (3)	-0.022 (2)	C(7)	0.018 (3)	0.021 (2)
N(2)	-0.030 (3)	-0.031 (2)	C(8)	0.000 (3)	-0.004 (2)
C(4)	0.015 (3)	0.017 (2)	C(9)	0.013 (3)	0.013 (2)
C(5)	0.017 (3)	0.016 (2)	D(8)	0.002 (4)	-0.002 (4)
C(6)	0.024 (3)	0.023 (2)	D(9)	0.028 (4)	0.027 (4)
P2: quinonoid ring					
10 <sup>-1</sup> MPa					
	139 (11)	-8340 (6)	5516	857 (65)	9.2
4.6 × 10 <sup>2</sup> MPa					
	135 (09)	-8351 (5)	5500	820 (54)	30.5
N(1)	-0.048 (3)	-0.044 (2)	C(7)	0.005 (3)	0.008 (2)
N(2)	-0.080 (3)	-0.083 (2)	C(8)	0.000 (3)	-0.002 (2)
C(4)	-0.011 (3)	-0.007 (3)	C(9)	0.000 (3)	-0.002 (2)
C(5)	-0.022 (3)	-0.025 (2)	D(8)	0.003 (4)	0.001 (4)
C(6)	-0.003 (3)	-0.003 (2)	D(9)	0.005 (4)	0.001 (4)

#### (b) TTF

	A	B	C	D	$\chi^2$
Q1: mean molecular plane (non-deuterium atoms)					
10 <sup>-1</sup> MPa					
	-181 (20)	9089 (6)	4166	0	171
4.6 × 10 <sup>2</sup> MPa					
	-132 (16)	9135 (16)	4066	0	226
S(1)	-0.027 (7)	-0.021 (6)	C(3)	-0.012 (3)	-0.015 (3)
S(2)	-0.024 (7)	-0.024 (6)	D(1)	0.012 (6)	0.014 (5)
C(1)	0.017 (3)	0.011 (3)	D(2)	0.018 (6)	0.016 (5)
C(2)	0.012 (3)	0.016 (3)			
Q2: central plane defined by C(3), S(1), S(2) and their centrosymmetric mates					
10 <sup>-1</sup> MPa					
	-194 (19)	9022 (23)	4308	0	0.5
4.6 × 10 <sup>2</sup> MPa					
	-127 (16)	9075 (20)	4199	0	7.5
S(1)	0.000 (7)	0.001 (6)	C(3)	-0.001 (6)	-0.005 (3)
S(2)	0.000 (7)	0.001 (6)	D(1)	0.077 (6)	0.072 (5)
C(1)	0.067 (3)	0.056 (3)	D(2)	0.081 (6)	0.076 (5)
C(2)	0.061 (3)	0.063 (3)			

lengths of S(1)–C(1) and S(2)–C(2) are found to be slightly unequal (0.02 Å) while Cooper, Kennedy, Edmonds, Nagel, Wudl & Coppens (1971) have observed with X-rays a difference of 0.03 Å for the neutral TTF molecule; (3) C(2)–C(3) has less double-bond character.

The TTF molecule is not planar (Table 5) but exhibits the chair conformation described elsewhere. The central part of the molecule, defined by S(1), S(2), C(3) and their centrosymmetrical mates, is planar, as is the exterior part defined by S(1), C(1), C(2), S(2). The angle ( $\approx 2.3^\circ$ ) between these planes does not change significantly with pressure.

The thermal ellipsoids of the atoms (Fig. 4) are similar at both pressures except for an average 9% decrease of the  $U_{ii}$  factors at  $4.6 \times 10^2$  MPa. The S atoms are an exception as their  $U_{11}$  parameters, surprisingly small at  $10^{-1}$  MPa, increase by 20% for S(1) and 80% for S(2) at  $4.6 \times 10^2$  MPa.

### (iii) Crystal packing

The crystal packings of TTF-TCNQ described from X-ray data (see Figs. 3 and 4 of Kistenmacher *et al.*, 1974) and neutron data are closely similar. The main structural parameters which characterize the stacking of molecules in columns of TTF and columns of TCNQ parallel to **b** are given in Table 6.

The effect of pressure on the crystal packing is mainly to reduce in the same way the distance between planes of TCNQ molecules [3.170 (3) Å at  $10^{-1}$  MPa; 3.104 (2) Å at  $4.6 \times 10^2$  MPa] and the distance between planes of TTF molecules [3.476 (2) Å at  $10^{-1}$  MPa; 3.417 (1) Å at  $4.6 \times 10^2$  MPa]. For TCNQ stacks, this change corresponds to the *b* contraction as the angle between the normal to the TCNQ mean molecular plane and **b** remains almost constant [34.03 (1)° at  $10^{-1}$  MPa; 33.91 (1)° at  $4.6 \times 10^2$  MPa]. For TTF stacks, the decrease in the interplanar spacing is accounted for by both the *b* contraction and a decrease of the angle that the normal to the TTF molecular mean plane makes with **b** [24.64 (3)° at  $10^{-1}$  MPa; 24.00 (3)° at  $4.6 \times 10^2$  MPa]. These small changes in the angles of tilt of the TTF and TCNQ molecules are within the e.s.d. of Friend, Miljak, Jérôme, Decker & Debray (1978) who found no change of the tilt angles under pressure from neutron powder data analysis.

In connection with these displacements, the overlap (ring-external-bond type) of molecules is slightly increased as shown by the pressure dependence of parameters  $\delta_y$  and  $\delta_z$  (Table 6).

As stated in earlier work there is no short intermolecular distance except for the S(1)···N'(2) and S(2)···N'(1) proximity between adjacent TTF and TCNQ molecules in the **a** direction. These S···N distances (Table 6), less than the sum of the van der

Waals radii of the atoms (3.35 Å), are unequal at room pressure and shorten to different extents when pressure increases. Chasseau, Gaultier, Hauw, Fabre, Giral & Torreilles (1978) have discussed the presence of a C(2)–H(2)···N(2) hydrogen bond between molecules of TTF and TCNQ adjacent in the [121] and [12̄1] directions. In fact, the C(2)···N(2) distance given in Table 6 of Kistenmacher *et al.* (1974) is in error (3.36 instead of 3.53 Å) and this hydrogen bond does not exist at room pressure and temperature. However, this C···N distance decreases by about 0.1 Å per  $5 \times 10^2$  MPa (Table 6) and therefore such a hydrogen bond (two per molecule) may exist in TTF-TCNQ if the pressure is high enough.

Table 6. Some geometrical characteristics of the molecules and of the crystal packing in TTF-TCNQ

The symbols used are defined as follows; TCNQ least-squares mean planes: *P*1 molecular plane (non-hydrogen or deuterium atoms), *P*2 quinonoid ring, *P*3 external plane [N(1), N(2), C(4), C(5), C(6)]; TTF least-squares mean planes: *Q*1 molecular plane (non-hydrogen or deuterium atoms), *Q*2 central plane [S(1), C(3), S(2) and their centrosymmetric mates], *Q*3 exterior plane [S(1), C(1), C(2), S(2)];  $\delta_y$ ,  $\delta_z$ : shifts of centre of mass in directions *y* of width and *z* of length of two overlapping molecules;  $l_1$ ,  $l_2$ : long axis of the *ac* projection of, respectively, the TTF molecule and the quinonoid ring of the TCNQ molecule. E.s.d.'s are given in parentheses.

	TTF-TCNQ (deuterated) <i>T</i> = 293 K (neutrons)		TTF-TCNQ (hydrogenated) <i>P</i> = $10^{-1}$ MPa (X-rays)	
	<i>P</i> = $10^{-1}$ MPa	<i>P</i> = $4.6 \times 10^2$ MPa	<i>T</i> = 300 K <sup>(1)</sup>	<i>T</i> = 100 K <sup>(2)</sup>
TCNQ				
<i>d</i> ( <i>P</i> 1 <i>P</i> 1) (Å)	3.170 (3)	3.104 (2)	3.168 (3)	3.113 (3)
<i>d</i> ( <i>P</i> 2 <i>P</i> 2) (Å)	3.190 (7)	3.124 (5)	3.188 (6)	3.132 (6)
( <i>P</i> 2, <i>P</i> 3) (°)	2.9 (2)	2.9 (1)	2.9 (1)	2.7 (1)
( <i>P</i> 1, <i>b</i> ) (°)	34.03 (1)	33.91 (1)	33.95 (1)	33.99 (1)
( <i>P</i> 2, <i>b</i> ) (°)	33.49 (3)	33.38 (3)	33.40 (3)	33.46 (3)
$\delta_y$ (Å)	0.087	0.087	0.083	0.082
$\delta_z$ (Å)	2.138	2.085	2.131	2.097
TTF				
<i>d</i> ( <i>Q</i> 1 <i>Q</i> 1) (Å)	3.476 (2)	3.417 (1)	3.473 (1)	3.426 (1)
<i>d</i> ( <i>Q</i> 2 <i>Q</i> 2) (Å)	3.451 (2)	3.395 (2)	3.451 (1)	3.402 (1)
( <i>Q</i> 2, <i>Q</i> 3) (°)	2.4 (3)	2.2 (2)	2.1 (1)	2.36 (7)
( <i>Q</i> 1, <i>b</i> ) (°)	24.64 (3)	24.00 (3)	24.58 (2)	24.12 (2)
( <i>Q</i> 2, <i>b</i> ) (°)	25.5 (1)	24.8 (1)	25.37 (3)	25.02 (1)
$\delta_y$ (Å)	0.019	0.003	0.014	0.019
$\delta_z$ (Å)	1.594	1.521	1.589	1.534
TTF and TCNQ				
( <i>P</i> 1, <i>Q</i> 1) (°)	58.62 (4)	57.88 (3)	58.49 (2)	58.07 (2)
N(2)···S(1) (Å)	3.245 (8)	3.172 (6)	3.249 (3)	3.186 (3)
N(1)···S(2) (Å)	3.199 (8)	3.148 (6)	3.203 (2)	3.153 (2)
N(2)···C(2) (Å)	3.518 (4)	3.424 (3)	3.521 (4)	3.436 (3)
N(2)···D(2) (Å)	2.524 (6)	2.428 (5)	1.00	0.94 (2)
N(2)···D(2)– C(2) (°)	151.4 (5)	151.1 (4)	150 (2)	152 (1.9)
( $l_1$ , $l_2$ ) (°)	1.08 (6)	0.99 (5)	1.08 (3)	0.89 (4)
( $l_1$ , <i>a</i> ) (°)	90.73 (6)	90.77 (5)	90.74 (4)	90.83 (3)
( $l_2$ , <i>a</i> ) (°)	91.80 (3)	91.76 (3)	91.82 (3)	91.72 (3)

Data in columns (1) and (2) have been recalculated from atomic coordinates provided respectively by Kistenmacher *et al.* (1974) and Blessing & Coppens (1974).

## (iv) Charge transfer

Flandrois & Chasseau (1977) have shown that the magnitude of the charge transfer may be estimated from the values of the bond lengths. Nevertheless, the parameterization proposed by these authors has been established from X-ray diffraction results and needs to be adapted to neutron data.

The main difference between X-ray and neutron results is due to the non-coincidence of the charge centroid and the nucleus of an atom. The magnitude of the shift is unknown both for the neutral molecule TCNQ<sup>0</sup> and for the ion TCNQ<sup>-</sup> but for TCNQ<sup>0</sup> it may be estimated from the results of Becker, Coppens & Ross (1973) on tetracyanoethylene. For this latter molecule the charge displacement is large only for the C atom of the cyanomethylene groups. It is 0.008, Å toward the N atom and thus will modify the average lengths of bonds *d* and *e* (Table 4), the first of which is used in the charge-transfer estimate (Fig. 5).

To confirm the role of this shift, neutron data on two other TCNQ salts are available, namely: (1) the 80 K structure of the complex of TCNQ with trimethylamine and iodine [TMA<sup>+</sup>.TCNQ<sup>2/3-</sup>.(I<sub>3</sub>)<sub>1/3</sub>] (Filhol & Gaultier, 1980); (2) the 40 K structure of a triethylammonium salt [TEA<sup>+</sup>.(TCNQ)<sub>2</sub><sup>-</sup>] (Filhol, Zeyen, Chenavas, Gaultier & Delhaes, 1980). Both are ion-radical salts with charge transfer equal to unity, but, from the stoichiometry, the charge on a TCNQ ion is 0.33 *e* for the first compound and has a mean value of 0.5 *e* for the second. For TTF-TCNQ the charge transfer is incomplete but is known to be 0.55 *e* at 300 K (Comès, Shapiro, Shirane, Garito & Heeger, 1975; Kagoshima, Ishiguro & Anzai, 1976; Khanna, Pouget, Comès, Garito & Heeger, 1977).

All these data are summarized in Fig. 5 and show that the difference between X-ray and neutron results is, as expected, mainly a decrease of the magnitude of *d-c*, while *b-c* changes little. There are, of course, still

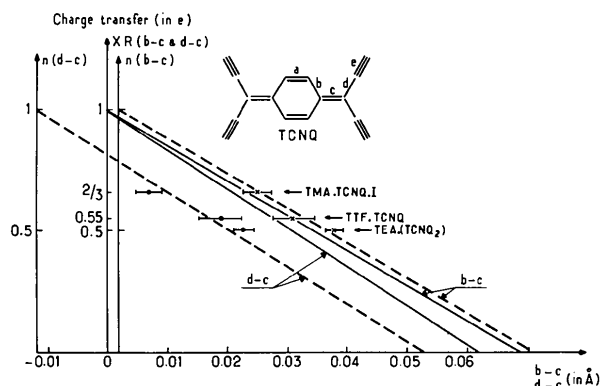


Fig. 5. Charge transfer as a function of bond length in TCNQ for neutron data. Continuous lines: X-ray results (Flandrois & Chasseau, 1977); broken lines: suggested law of variation for neutron data.

some doubts about the exact slope and position of the broken lines *b-c* and *d-c* drawn on Fig. 5 but it is encouraging to find that, with the present data set, the charge displacement is larger for TCNQ<sup>-</sup> ( $\approx 0.012$  Å) than for TCNQ<sup>0</sup> ( $\approx 0.008$ , Å) because this is consistent with the fact that charges are localized on the C≡N bonds.

In any case, the relative change of the charge transfer in TTF-TCNQ between  $10^{-1}$  and  $4.6 \times 10^2$  MPa at room temperature is not very sensitive to the above uncertainty and is found to be 10% from data in Table 4 and Fig. 5. Thus the corresponding charge transfer at  $4.6 \times 10^2$  MPa is 0.61 *e*. At 10 K, Megtert *et al.* (1979) have shown that a pressure of  $5 \times 10^2$  MPa increases the charge transfer by only 4%. These two latter percentages are roughly in the same ratio as the compressibilities of the *b* axis of the cell at the corresponding temperatures ( $\Delta b/b = -0.6 \times 10^{-4}$  MPa<sup>-1</sup> at 300 K,  $\Delta b/b = -0.26 \times 10^{-4}$  MPa<sup>-1</sup> at 10 K according to Megtert *et al.*, 1979). This is in agreement with the simple hypothesis that the *b*-axis strain contribution to the pressure dependence of the charge transfer is predominant because of its direct effect on the bandwidth (Jérôme, 1977).

## (v) Rigid-body thermal vibrations

A rigid-body analysis (Schomaker & Trueblood, 1968) of the thermal parameters has been made. The observed directions of the principal axes of translational and rotational vibrations of the TTF and TCNQ molecules are close to the molecular inertial axis, as observed in other similar compounds.

For the TCNQ molecule, the corresponding amplitudes are in agreement with X-ray results at 100 and 60 K (Schultz *et al.*, 1976) with, however, a larger anisotropy. For the TTF molecule, the direction of highest translation and libration amplitudes is not the long axis of the molecule, as expected, but is almost the normal to the molecular plane. This indicates that a bias may exist in the thermal parameters although no obvious anomaly, except perhaps for the S atoms, is visible on thermal-ellipsoid plots (Fig. 4).

## Compressibility and thermal expansion of TTF-TCNQ

## (i) Compressibility

The compressibility of TTF-TCNQ has been measured (Debray, Millet, Jérôme, Barišić, Giral & Fabre, 1977) up to  $20 \times 10^2$  MPa by powder neutron diffraction techniques and by Welber, Seiden & Grant (1978) up to  $70 \times 10^2$  MPa, with single-crystal optical measurements. More recently a two-axis neutron spectrometer study (Megtert *et al.*, 1979) gave *a* sin  $\beta$  and *b* compressibilities in disagreement with earlier work by about 25%.

To clarify this point, the cell dimensions of deuterated TTF-TCNQ have been measured at room temperature and in the pressure range  $10^{-1}$  to  $4.6 \times 10^2$  MPa (Table 1) on the D8 four-circle neutron diffractometer. The compressibility coefficients thus obtained [ $\kappa_a = 0.18(1) \times 10^{-4}$ ,  $\kappa_b = 0.59(1) \times 10^{-4}$ ,  $\kappa_c = 0.13(1) \times 10^{-4}$  MPa $^{-1}$ ] corroborate those of Megtert *et al.* (1979). The bulk modulus ( $B = \kappa_v^{-1}$ ) and its derivative ( $B'$ ) fitted through the Murnaghan equation of state

$$P = \frac{B}{B'} \left[ \left( \frac{V_0}{V} \right)^{B'} - 1 \right]$$

are  $B = 114(2)$ ,  $B' = 6(1) \times 10^2$  MPa.

The directions ( $\mathbf{k}_i$ ) and magnitude [ $k_i = (1/l)(dl/dp)$ ] of the principal compressibilities have also been calculated (Fig. 6). Because TTF-TCNQ is monoclinic, the  $b$  axis of the cell is a principal axis ( $\mathbf{k}_b$ ) while  $\mathbf{k}_1$  and  $\mathbf{k}_3$  lie in the  $ac$  plane. These calculations show that the anisotropy of TTF-TCNQ with respect to strain is, at room pressure, in the ratio 0.67:2.00:0.33 and thus somewhat larger than was believed up to now. The crystal will become nearly isotropic at about  $10^3$  MPa because of the fall-off of  $k_b$  when pressure increases while  $k_1$  and  $k_3$  remain practically constant. Another interesting point is that the direction of the minimal compressibility ( $\mathbf{k}_3$ ) is approximately parallel to the [101] direction and slightly rotates toward the  $a$  axis when pressure increases.

### (ii) Thermal expansion

The thermal expansion of TTF-TCNQ has already been studied by Schultz *et al.* (1976) by X-ray diffraction and also by Schafer, Thomas & Wudl (1975), for the  $b$  axis only, with a capacitance dilatometer. Both studies were essentially oriented

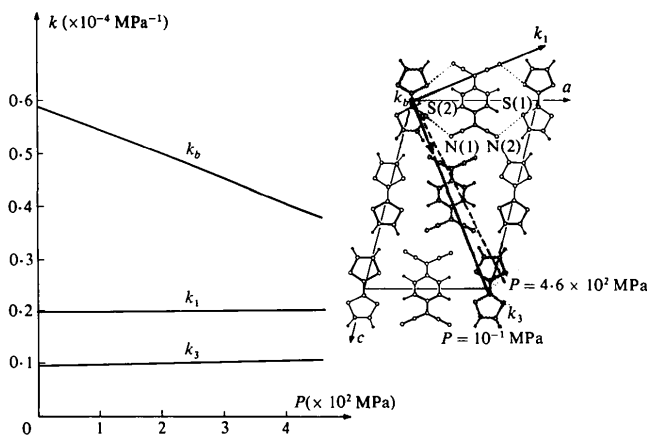


Fig. 6. Principal compressibilities  $k_i = -(1/l_i)(dl_i/dp)$  and their directions as a function of pressure.

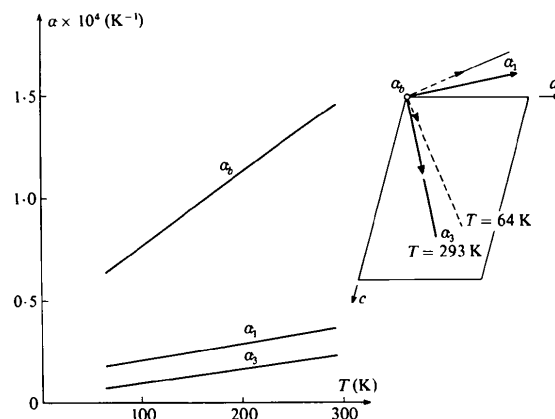


Fig. 7. Principal thermal expansions  $\alpha_i = (1/l_i)(dl_i/dp)$  and their directions as a function of pressure.

toward the detection of anomalies in the cell parameters at the temperature of the metal-insulator transition of TTF-TCNQ and do not provide an accurate set of data for the high-temperature phase.

The cell dimensions given in Table 1 for the temperature range 64 to 293 K were obtained on the same sample of deuterated TTF-TCNQ as all the other data in this paper. They are in good agreement with earlier results and lead to thermal-expansion coefficients at room temperature [ $\alpha_a = 0.37(3) \times 10^{-4}$ ,  $\alpha_b = 1.47(8) \times 10^{-4}$ ,  $\alpha_c = 0.27(4) \times 10^{-4}$ ,  $\alpha_{\text{vol}} = 2.09(9) \times 10^{-4}$  K $^{-1}$ ] somewhat different from the values derived from an inadequate data set (e.g.:  $\alpha_{\text{vol}} = 1.5 \times 10^{-4}$  K $^{-1}$ , Zallen & Conwell, 1979).

The directions ( $\alpha_i$ ) and magnitude [ $\alpha_i = (1/l_i)(dl_i/dT)$ ] of the principal expansion have been calculated (Fig. 7). They show that the expansion anisotropy at room temperature is in the ratio 0.54:2.12:0.34 and is thus of the same order of magnitude as the compressibility anisotropy. The expansion is a minimum ( $\alpha_3$ ), as expected, in a direction which is close to the [101] axis. If temperature decreases  $\alpha_3$  slightly rotates toward a as  $\mathbf{k}_3$  does when pressure increases.

### (iii) Discussion

The anisotropy of elastic properties exhibited by TTF-TCNQ is weak with respect to the anisotropy of its electronic properties. At first sight its compressibility is not very different from that of organic van der Waals solids as noted by Zallen & Conwell (1979) (e.g.: naphthalene  $\kappa_v = 1.64 \times 10^{-4}$ , anthracene  $\kappa_v = 1.42 \times 10^{-4}$  MPa $^{-1}$ ).

Following Vaidya & Kennedy (1971), who showed that compressibility of organic compounds is a function of the ratio of intramolecular covalent forces to intermolecular forces, it may be possible to characterize better the crystal-packing interactions in TTF-TCNQ. This may be achieved by comparing the bulk

modulus of TTF–TCNQ [or even its relative volume extrapolated to  $45 \times 10^2$  MPa ( $V/V_0 \approx 0.81$ ) by means of the Murnaghan equation] versus half the molar volume (two covalent entities in the molecule) to data given in Table II or Fig. 2 of Vaidya & Kennedy (1971). This indicates that, at *equal molar volume*, the bulk compressibility of TTF–TCNQ is larger than that of van der Waals compounds such as naphthalene or anthracene, is in the range of that of aromatic compounds substituted with halogen atoms, and is less than the compressibility of polar molecules such as nitramines (Filhol, Rey-Lafon & Bravic, 1981). This is in agreement with the results of theoretical calculations (Grovers, 1978) giving a contribution of the electrostatic energy to the total lattice energy of about 40%.

Furthermore, the magnitudes and directions of the principal compressibilities reflect the arrangement of the molecular ions in the crystal.

Indeed it is striking to find that the direction of minimum compressibility ( $k_3$ ) is neither **a** nor **c** but [101] (Fig. 6), *i.e.* the direction along which the TTF and TCNQ molecules align and alternate on an *ac* projection of the structure. In fact, these alignments of molecules are not in the *ac* plane but in either the [121] or the [ $\bar{1}21$ ] directions, alternately along **a** (Fig. 8). They correspond to molecules roughly coplanar (out-of-plane distance  $< 0.5$  Å) thus constituting *crossing strips bearing a high density of atoms*. The internal and external bisectors of the [121] and [ $\bar{1}21$ ] directions are respectively the [101] and **b** directions which are precisely those of the principal compressibilities  $k_3$  and  $k_b$ . Finally, the [121] and [ $\bar{1}21$ ] strips form segregated stacks thus constituting *parallel layers* [planes (**b**, [121]) and (**b**, [ $\bar{1}21$ ])] with thickness roughly the mean width of TTF and TCNQ molecules.  $k_1$  is nearly normal to these layers.

The above description accounts qualitatively for the directions of the principal compressibilities at room pressure. Thus, as no large reorientation of molecules occurs under pressure, the effect of strain on the crystal packing may be crudely split up as follows: (i) The layers of staggered strips are brought closer together along the direction of their normal. (ii) There is a

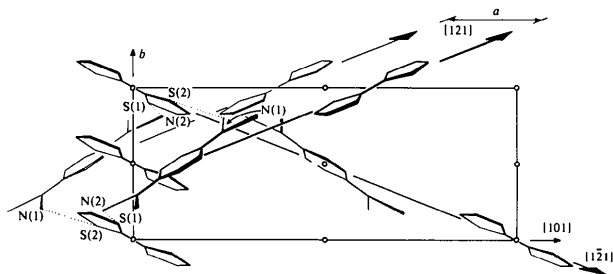


Fig. 8. The structure of TTF–TCNQ viewed in projection on the (**b**, [121]) plane.

shearing of one type of layer relative to the other, corresponding to a change of  $-0.00192$  ( $5^\circ$ ) per MPa in the angle between directions [121] or [ $\bar{1}21$ ]. (iii) Within a layer there is a shrinking of the axes [121] or [ $\bar{1}21$ ] corresponding to TTF and TCNQ molecules coming closer together within the strips and a decrease of the stacking distance of the strips.

It is now possible to explain qualitatively the compressibility anisotropy. If it is assumed that the intermolecular interactions are isotropic, if no molecular deformation or reorientation occurs under pressure, then the compressibility in a given direction is inversely proportional to the mean size of the molecules in that direction.\* For TTF–TCNQ this leads to a calculated anisotropy (0.9:1.6:0.5) slightly smaller than the observed one (0.67:2.0:0.33).

We suggest that the above discrepancy between observed and calculated anisotropies is mainly due to the anisotropy of the intermolecular interactions in TTF–TCNQ. This suggests that interactions along **b** (and thus the overlap of molecular orbitals in this direction) are the most sensitive to pressure. In this connection, it may be noted that  $\kappa_{[121]} = 0.16 \times 10^{-4}$  and  $\kappa_a = 0.18 \times 10^{-4}$  MPa $^{-1}$  have similar values which, considering the shape of the molecules, suggests that the intermolecular interactions are larger along **a** than along [121]. This is again in agreement with a result of the analysis of the structure, namely that the anionic and cationic stacks are strongly coupled in the **a** direction *via* the short S...N contacts.

Therefore, the observation  $\kappa_c < \kappa_a$  is only in apparent contradiction to the existence of this strong interchain coupling and this shows that the interpretation of compressibilities in terms of intermolecular interaction is not straightforward.

The analysis of the variation of the cell dimensions with temperature leads to principal directions and anisotropies of thermal expansion which, at room temperature, are similar to those observed for compressibilities. Therefore, the above simple model developed to explain compressibility also explains the thermal expansion of TTF–TCNQ. This is not surprising because the strength and anharmonicity of the intermolecular interactions are not independent and the shape and size of the molecules have the same large effect on both compressibility and thermal expansion, at least for van der Waals crystals. At low temperature the anisotropy of the crystal is similar to that observed at room temperature.

Compressibility and thermal-expansion data from earlier works have been used in several papers in the calculations of some physical properties of TTF–TCNQ. In the following, three examples are given of the effect of the use of our new data.

\* This simple model has been used with success for polyphenyls (Ecolivet & Sanquer, 1980).

The value of the Grüneisen constant ( $\gamma$ ) of TTF-TCNQ may be calculated by two different formulae:

$$\gamma = B(T)V_m(T)\alpha_v(T)/C_v(T), \quad (1)$$

$$\gamma = \frac{V\partial^2 V/\partial P^2}{2(\partial V/\partial P)^2} - \frac{2}{3}, \quad (2)$$

where  $V$  is the volume of the unit cell,  $V_m$  the molar volume,  $\alpha_v$  the thermal expansion,  $B$  the bulk modulus,  $C_v$  the heat capacity at constant volume related to  $C_p$ , the specific heat at constant pressure, by  $C_p - C_v = \alpha_v^2 B V_m T$ . For TTF-TCNQ only low-temperature  $C_p$  data are available and therefore calculations with (1) have been made for  $T = 64$  K using  $C_p(64 \text{ K})/R = 16.7$  (Craven, Salomon, De Pasquali, Herman, Stucky & Schultz, 1974; Djurek, Franulović, Prester, Tomić, Giral & Fabre, 1977) and  $B(64 \text{ K}) = 168 \times 10^2$  MPa. This latter value has been estimated by linear interpolation between 10 and 300 K data (Megtert *et al.*, 1979), the change in elastic properties at the transition temperature (Teidje, Haering, Jericho, Roger & Simpson, 1977) being neglected. The value of the Grüneisen constant of TTF-TCNQ is then:  $\gamma = 2.7$  from (1) and  $\gamma = 2.3$  (5) from (2), values consistent with  $\gamma = 2.56$  obtained by Teidje *et al.* (1977) from sound-velocity measurements, while data of Debray *et al.* (1977) give  $\gamma = 1.6$  from (2).

Temperature has an effect upon libron frequencies by changing both the phonon occupation numbers at fixed equilibrium positions of atoms (phonon-excitation-driven effect) and the equilibrium interatomic spacing (volume-driven effect). The relative contribution of these effects is given by  $\eta = (\alpha_v/\kappa_v)(\partial T/\partial P)_v$ , with  $\eta$  lying in the range 0.5 to 1.5 for a number of molecular crystals (Zallen & Conwell, 1979), thus indicating a dependence of external mode frequencies dominated by the volume-driven effect. For TTF-TCNQ these authors gave  $\eta = 1.5$ , a value which changes to  $\eta = 2.5$  if  $\alpha_v$  and  $\kappa_v$  from the present work are used. Therefore, at room temperature, TTF-TCNQ shows a substantial phonon-excitation-driven contribution to the libron frequencies, a behaviour which thus differs from that of aromatic compounds such as anthracene and pyrene.

Bouffard & Zuppiroli (1978) have measured the elastoresistivity of TTF-TCNQ by a novel strain-gauge technique. They gave an estimate of the effects on the longitudinal and transverse resistivities of an elementary uniaxial strain applied along one of the three axes  $a$ ,  $b$  or  $c^*$ . The fraction of longitudinal piezoresistivity attributable, in a hydrostatic experiment, to transverse effects was found to be  $43 \pm 10\%$  of the total value. With the compressibility data of the present study, this latter value reduces to  $23 \pm 13\%$  (Bouffard, 1980) and is then in better agreement with the ideas of Jérôme (1977).

## Conclusion

Up to now very few structures of molecular crystals have been measured at high pressure. We believe that the structure of TTF-TCNQ at  $4.6 \times 10^2$  MPa is one of the first high-pressure structures of an organic crystal measured on a four-circle neutron diffractometer. This work shows that, even for large molecules, data obtained with an Al cell are of good quality.

Some major results of this study of the effect of pressure on the structure of TTF-TCNQ are the following. The principal crystal-packing modification is a decrease in the stacking distances of molecules in the TTF and TCNQ columns, the effect of  $4.6 \times 10^2$  MPa of hydrostatic pressure (Table 5) being equivalent to the effect of a temperature decrease from 300 to about 80 K. The reorientation of molecules with respect to the cell axes  $a$  and  $b$  is small, the larger value  $[-0.6 (1^\circ)]$  being observed for the tilt angle of the TTF mean molecular plane with respect to  $b$ . The short S...N intermolecular distances reduce with pressure with a tendency to become equal. Finally, an increase of the charge transfer of about 10% for  $4.6 \times 10^2$  MPa has been deduced from the change in the intramolecular bond lengths.

At room temperature and room pressure, the thermal expansion and compressibilities of TTF-TCNQ have ratios of longitudinal over transverse values less than or equal to 6. For the compressibility this ratio decreases rapidly when pressure increases, while for thermal expansion it remains nearly constant with temperature. Both these physical properties show that the intermolecular forces in TTF-TCNQ are strongly anharmonic in the  $b$  direction and much less in the  $ac$  plane. Both also have principal axes of similar directions, directions which may be understood through a simple model based on structural considerations.

It is now tempting to extrapolate these results toward higher pressures and thus toward higher values of charge transfer, especially because Friend, Miljak & Jérôme (1978) have shown that, at 70 K and  $17 \times 10^2$  to  $21 \times 10^2$  MPa, there is a locking of the charge-density waves which corresponds to a charge transfer of  $\frac{2}{3}e$ . From the data of the present work, such a charge transfer would be reached *at room temperature* under a pressure of about  $10\text{--}12 \times 10^2$  MPa. At this pressure, the short distances S(1)...N(2) and S(2)...N(1) between atoms of TTF and TCNQ molecules adjacent in the  $a$  direction would have equal lengths; the hydrogen bonds C(2)—D(2)...N(2) between TTF and TCNQ molecules in the [121] and  $[\bar{1}21]$  directions would be of appreciable strength; the compressibility anisotropy of the crystal would be a minimum.

This work was suggested by Professor R. Comès (Laboratoire de Physique des Solides, Université de Paris-Sud, France). The authors thank Professor A. F.

Garito (Department of Physics and Laboratory for Research on the Structure of Matter, University of Pennsylvania, USA) who supplied the single crystals, Professor Lajz erowicz (Laboratoire de Spectrom trie Physique, Facult  des Sciences de Grenoble, France) for instructive discussions on thermal expansion and compressibility in molecular crystals, Dr D. Watkin (Chemical Crystallography Laboratory, Oxford, England) for his help in reducing the data, and Dr S. A. Mason for checking the manuscript.

*Note added in proof:* The original powder data of Debray *et al.* (1977) were re-examined and the cell dimensions calculated using our programs were found to be somewhat different from their published values. The recalculated compressibilities ( $\kappa_a = 0.19 \times 10^{-4}$ ,  $\kappa_b = 0.51 \times 10^{-4}$ ,  $\kappa_c = 0.14 \times 10^{-4}$  MPa $^{-1}$  at  $P = 10^{-1}$  MPa and  $\kappa_a = 0.10 \times 10^{-4}$ ,  $\kappa_b = 0.18 \times 10^{-4}$ ,  $\kappa_c = 0.11 \times 10^{-4}$  MPa $^{-1}$  at  $P = 15 \times 10^2$  MPa) are then in much better agreement with our values. Furthermore the corresponding axes of the principal compressibilities have new directions similar to those shown on Fig. 6 and a rotation of  $\mathbf{k}_3$  towards  $\mathbf{a}$  of about  $24^\circ$  is observed when the pressure is increased to  $15 \times 10^2$  MPa. Although this recalculation leads to a better overall agreement with our data, discrepancies still remain (Gr neisen constant  $\gamma \sim 1.6$ ,  $\kappa_b$  and anisotropy, smaller than ours) which may be only partially explained by an overestimate of the pressure ( $\sim 15\%$ ) in the powder experiments.

#### References

- ALBERTSSON, J., OSKARSSON, A. & ST HL, K. (1978). *Acta Cryst.* **A34**, S343.
- ALLIBON, J. R., FILHOL, A., LEHMANN, M. S., MASON, S. A. & SIMMS, P. (1981). *J. Appl. Cryst.* In the press.
- BECKER, P., COPPENS, P. & ROSS, F. K. (1973). *J. Am. Chem. Soc.* **95**, 7604–7608.
- BLESSING, R. H. & COPPENS, P. (1974). *Solid State Commun.* **15**, 215–221.
- BOUFFARD, S. (1980). Private communication.
- BOUFFARD, S. & ZUPPIROLI, L. (1978). *Solid State Commun.* **28**, 113–117.
- CHASSEAU, D., GAULTIER, J., HAUW, C., FABRE, J. M., GIRAL, L. & TORREILLES, E. (1978). *Acta Cryst.* **B34**, 2811–2818.
- COM S, R., SHAPIRO, S. M., SHIRANE, G., GARITO, A. F. & HEEGER, J. (1975). *Phys. Rev. Lett.* **35**, 1518–1521.
- COOPER, W. F., KENNEDY, N. C., EDMONDS, J. W., NAGEL, A., WUDL, F. & COPPENS, P. (1971). *Chem. Commun.* pp. 889–890.
- CRAVEN, R. A., SALAMON, M. B., DE PASQUALI, G., HERMAN, R. M., STUCKY, G. & SCHULTZ, A. (1974). *Phys. Rev. Lett.* **32**, 769–772.
- DEBRAY, D., MILLET, R., J R ME, D., BARI IĆ, S., GIRAL, L. & FABRE, J. M. (1977). *J. Phys. (Paris) Lett.* **38**, L227–L231.
- DJUREK, D., FRANULOVIC, K., PRESTER, M., TOMIĆ, S., GIRAL, L. & FABRE, J. M. (1977). *Phys. Rev. Lett.* **38**, 715–718.
- ECOLIVET, C. & SANQUER, M. (1980). *J. Chem. Phys.* **72**, 4145–4152.
- FILHOL, A. & GAULTIER, J. (1980). *Acta Cryst.* **B36**, 592–596.
- FILHOL, A., REY-LAFON, M. & BRAVIC, G. (1981). To be published.
- FILHOL, A., ZEYEN, C. M. E., CHENAVAS, P., GAULTIER, J. & DELHAES, P. (1980). *Acta Cryst.* **B36**, 2719–2726.
- FLANDROIS, S. & CHASSEAU, D. (1977). *Acta Cryst.* **B33**, 2744–2750.
- FRIEND, R. H., MILJAK, M. & J R ME, D. (1978). *Phys. Rev. Lett.* **40**, 1048–1051.
- FRIEND, R. H., MILJAK, M., J R ME, D., DECKER, D. L. & DEBRAY, D. (1978). *J. Phys. (Paris) Lett.* **39**, L134–L138.
- GROVERS, H. A. J. (1978). *Acta Cryst.* **A34**, 960–965.
- J R ME, D. (1977). *J. Phys. (Paris) Lett.* **38**, L489–L494.
- JOHNSON, C. K. (1965). *ORTEP*. Report ORNL-3794. Oak Ridge National Laboratory, Tennessee.
- KAGOSHIMA, S., ISHIGURO, T. & ANZAI, H. (1976). *J. Phys. Soc. Jpn.* **41**, 2061–2071.
- KHANNA, S. K., POUGET, J. P., COM S, R., GARITO, A. F. & HEEGER, A. J. (1977). *Phys. Rev. B*, **16**, 1468–1479.
- KISTENMACHER, T. J., PHILLIPS, T. E. & COWAN, D. O. (1974). *Acta Cryst.* **B30**, 763–768.
- MEGIERT, S., COM S, R., VETTIER, C., PYN, R. & GARITO, A. F. (1979). *Solid State Commun.* **31**, 977–980.
- PAUREAU, J. (1980). Unpublished results.
- PAUREAU, J. & VETTIER, C. (1975). *Rev. Sci. Instrum.* **46**, 1484–1488.
- SCHAFFER, D. E., THOMAS, G. A. & WUDL, F. (1975). *Phys. Rev. B*, **12**, 5532–5535.
- SCHOMAKER, V. & TRUEBLOOD, K. N. (1968). *Acta Cryst.* **B24**, 64–76.
- SCHULTZ, A. J., STUCKY, G. D., BLESSING, R. H. & COPPENS, P. (1976). *J. Am. Chem. Soc.* **98**, 3194–3201.
- STEWART, J. M. (1974). The XRAY system. Computer Science Center, Univ. of Maryland, College Park, Maryland.
- TEIDJE, T., HAERING, R. R., JERICHO, M. H., ROGER, W. A. & SIMPSON, A. (1977). *Solid State Commun.* **23**, 713–718.
- VAIDYA, S. N. & KENNEDY, G. C. (1971). *J. Chem. Phys.* **55**, 987–992.
- WASER, J., MARSH, R. E. & CORDES, A. W. (1973). *Acta Cryst.* **B29**, 2703–2708.
- WELBER, B., SEIDEN, P. E. & GRANT, P. M. (1978). *Phys. Rev. B*, **18**, 2692–2700.
- ZALLEN, R. & CONWELL, E. M. (1979). *Solid State Commun.* **31**, 557–561.